International Immunopharmacology 72 (2019) 195–203

Contents lists available at ScienceDirect

International Immunopharmacology

journal homepage: www.elsevier.com/locate/intimp

Daphnetin prevents methicillin-resistant *Staphylococcus aureus* infection by inducing autophagic response

Wei Zhang[a,1], Shiqin Zhuo[b,1], Long He[a], Cheng Cheng[a], Bo Zhu[a], Yin Lu[c], Qinan Wu[d], Wenbin Shang[e], Weihong Ge[b], Liyun Shi[a,*]

[a] School of Medicine and Life Science, Nanjing University of Chinese Medicine, Nanjing 210046, China
[b] School of Pharmaceutics, Zhejiang Chinese Medical University, Zhejiang 310053, China
[c] Jiangsu Key Laboratory for Pharmacology and Safety Evaluation of Chinese Materia Medica, School of Pharmacy, Nanjing University of Chinese Medicine, Nanjing 210023, China
[d] Collaborative Innovation Center of Chinese Medicinal Resources Industrialization, Nanjing 210023, China
[e] The First School of Clinical Medicine, Nanjing University of Chinese Medicine, Nanjing 210023, China

ARTICLE INFO

Keywords:
Staphylococcus aureus
Pneumonia
Daphnetin
Autophagy

ABSTRACT

The bacterial pneumonia caused by methicillin-resistant *Staphylococcus aureus* (MRSA) is a potentially fatal disease, featured with extensive infection, inflammation, and airway dysfunction. With the increasing emerging of drug-resistant strains, new therapeutic strategies beyond canonical antibiotic treatment are pressingly needed. Daphnetin (DAPH) is a natural coumarin derivative with anti-inflammation, anti-microorganism and anti-oxidative properties. However, the protective effect of DAPH on *S. aureus*-caused pneumonia and the mechanism involved are never explored. Here we show that DAPH treatment conferred substantial protection against *S. aureus*-induced pneumonia, characterized by the reduced inflammatory responses, the augmented bacterial clearance and the alleviated tissue damage. Our study indicates that DAPH significantly enhanced mTOR-dependent autophagic pathway, leading to the boosted microphage bactericidal activity and the suppressed inflammatory responses. Inhibition of autophagic pathway therefore largely abolished DAPH-elicited repression of inflammatory response and macrophage anti-bacterial capability. Together, we herein not only identify a novel, natural agent to combat bacterial pneumonia, but also underscore the significance of autophagic pathway in orchestrating antimicrobial and anti-inflammatory responses, which may have important implication for the treatment of the infectious diseases, particularly that caused by obstinate, antibiotic-resistant pathogens such as MRSA.

1. Introduction

Staphylococcus aureus (*S. aureus*) is a ubiquitous pathogen causing a wide spectrum of infections ranging from skin and soft tissue infection to sepsis, bacteremia, endocarditis, meningitis, and pneumonia. The pathogen has evolved multiple virulence factors such as Panton-Valentine leukocidin, α-hemolysin, and protein A that make it one of the most invasive and pathogenic agents worldwide [1–3]. Moreover, extensive inflammation, tissue damage, and progressive organ dysfunction during infection have been proved to causatively relate with high mortality of staphylococcal infection, particularly critical infection such as staphylococcal pneumonia. Acute lung injury (ALI) that was featured with abundant neutrophil infiltration, cytokines release, and permeability pulmonary edema, would lead to diffuse alveolar damage and low lung compliance. Furthermore, with the widespread use of antibiotics, there is increasing emergence and prevalence of strains resistant to every clinically available antibiotic, such as methicillin-resistant *S. aureus* (MRSA) [4]. Pneumonia and ALI caused by *S. aureus* have been identified as a major cause of in-hospital mortality from the multiple-organ dysfunction syndrome (MODS) [5]. Considering the fact that high mortality of staphylococcal pneumonia is frequently intertwined with aberrant inflammation and uncontrolled infection,

Abbreviations: S. aureus, *Staphylococcus aureus*; DAPH, daphnetin; MRSA, methicillin-resistant Staphylococcus aureus; CFU, Colony Forming Unit; ALI, acute lung injury; MODS, multiple-organ dysfunction syndrome; DCs, dendritic cells; Treg, regulatory T; BALF, bronchoalveolar lavage fluid; MOI, multiplicity of infection; TFEB, transcription factor EB; i.p., intraperitoneal; i.t., intratracheal; MPO, myeloperoxidase; DMSO, Dimethyl sulfoxide

* Corresponding author.
E-mail address: shi_liyun@msn.com (L. Shi).
[1] These authors contributed equally to this work.

https://doi.org/10.1016/j.intimp.2019.04.007
Received 18 January 2019; Received in revised form 25 March 2019; Accepted 3 April 2019
Available online 13 April 2019
1567-5769/

therapies that coordinate host responses to these two processes might bring new promise for treating staphylococcal pneumonia, when compared with current antibiotic treatment.

Autophagy is a highly conserved intracellular process that delivers cytoplasmic components to the autophagosome and lysosome for degradation. The autophagic process is thereby viewed as a crucial mechanism for maintaining cellular and tissue homeostasis [6,7]. During this process, cytosolic components, such as organelles and long-lived proteins, are sequestered into a double-membrane autophagosome, which would subsequently fuse with the lysosomes to form an autolysosome for the degradation of the enclosed material. Autophagy has long been regarded as a key cytoplasmic quality control mechanism to eliminate protein aggregates and damaged organelles. However, increasing data indicate that cellular autophagy also serves as a crucial host defensive response by delivering intracellular pathogens to the lysosomes for lysis and eradication [8]. The invading pathogens uptaken by macrophages haven been shown to be transported and internalized into phagosomes, or cytoplasmic bacteria are captured by autophagy machinery and delivered into autophagosome. These enclosed pathogens would then be delivered to lysosomes or autolysosomes where they are destroyed. Besides, the autophagic process exerts the regulatory effects on the induction and modulation of inflammatory reactions, presumably through devouring the inflammatory ligands or interfering the inflammatory signaling. Defective autophagy is associated with extensive inflammapathology and severe inflammatory diseases [9–12]. Because cellular autophagy has an important role in both inflammatory and immune responses, the agents targeting cellular autophagy are increasingly emerging as new anti-infectious treatments [13].

Daphnetin (7, 8-dihydroxycoumarin, DAPH) is a natural coumarin derivative isolated from plants of the genus Daphne that has been clinically used to treat a variety of inflammatory diseases, such as rheumatoid arthritis and coagulation disorders. DAPH possess a variety of biological properties, including anti-inflammation, anti-oxidative stress, antimicrobial, and anticancer activity [14–16]. Studies from our lab and other investigators indicated that DAPH can potentially promote the development of regulatory T (Treg) while inhibiting the differentiation of inflammatory Th17 and Th1 cells [17,18]. Also, it exhibited the ability to suppress the activation and maturation of dendritic cells (DCs), suppressing the differentiation of proinflammatory Th17 cells and hence contributing to the lessened experimental autoimmune encephalomyelitis (EAE) [19]. Our recent data showed that DAPH substantially dampened the NF-κB-driven inflammatory signaling through modulating the activity of the ubiquitin-editing enzyme A20 and the subsequent TRAF6 activity, leading to the alleviated airway inflammation and the protection of endotoxin-induced ALI [16]. These studies point to DAPH as a potent regulator of immune and inflammatory responses, but its relevance to bacterial pneumonia and to autophagic pathway is yet to be determined.

In the present study, we reveal that DAPH treatment provided a profound protection against *S. aureus*-induced lung inflammation and injury. DAPH significantly enhanced macrophage bactericidal activity while repressing inflammatory responses mainly through boosting mTOR-dependent autophagic pathway. This finding extends our understanding about anti-bacterial autophagy and DAPH, and suggests an alternative therapeutics for the obstinate pathogens such as MRSA.

2. Materials and methods

2.1. Reagents and antibodies

DAPH (S2554) was purchased from Selleck Chemicals China (Shanghai). Cell Counting Kit-8 (CCK8, C0038) was obtain from Beyotime Institute of Biotechnology. The *S. aureus* strain was a clinical isolate from the Second Affiliated Hospital, Zhejiang University, and its identification was confirmed by biochemical assays (the Vitek 2 compact system, bioMerieux) and 16S ribosomal RNA gene sequencing.

Antibodies (Abs) specific for total and phosphorylated forms of p38 (Thr180/Tyr182), ERK1/2 (Thr202/Tyr204), JNK (Thr183/Tyr185), p65 (Ser536), IKKα/β (Ser176), IκBα (Ser32), mTOR (Ser2448), p70S6 Kinase (Thr421/Ser424), 4E-BP1 (Thr37/46) and ULK1 (Ser757) were obtained from Cell Signaling Technology (Beverly, MA). Abs against LC3A/B (#4108), LC3B (#3868) and β-actin (#4970) were obtained from Cell Signaling Technology (Beverly, MA).

2.2. Colony forming unit (CFU)

RAW264.7 cells (5×10^5) were seeded in six-well plates, after infection for 4 h (multiplicity of infection [MOI], 10), cells were washed with sterile PBS and added new complete medium (10% FBS) into the plates in the presence or absence of DAPH (160 μM). After 48 h, the cells were ruptured (0.1% Triton X-100) to release intracellular bacteria and diluted to appropriate dilutions with sterile PBS for CFU count on 7H10 agar plates.

To determine the bacteria burden in lung and blood, whole blood of mice was collected into 1.5 mL Eppendorf tubes containing 2 μL of heparin (20 units/mL). Lung tissue homogenate and whole blood were diluted and applied evenly to the plate for CFU count.

2.3. Cell viability

RAW264.7 cells (1×10^4) were seeded into 96-well culture plates overnight at 37 °C and atmospheric conditions of 5% CO_2. The culture medium was then replaced with medium containing different concentrations of DAPH (40, 80, 160 μM) for 24 h. At the end of the culture, 10 μL of the CCK-8 reagent was added to each well. After 1–2 h of incubation at 37 °C, the absorbance was determined at 450 nm using a Synergy 2 Microplate Reader (Bio-Tek, USA).

2.4. ROS production assay

ROS production was assayed using DCFH-DA by following a protocol provided by the manufacturer (Beyotime). The cells were rinsed with serum-free medium (SFM) 3 times and then were fed with DCFH-DA fluorescent probe (at 5 μM) in fresh SFM for another hour. At the end of incubation, the cells were washed 3 times with PBS and collected by trypsin-EDTA treatment. ROS production was measured by flow cytometry with an excitation wavelength of 488 nm and emission wavelength of 525 nm. FlowJo software was used to determine fluorescence-positive cells and the MFI.

2.5. Immunofluorescence staining

Cells were grown on cover glasses, fixed with 4% paraformaldehyde, and permeabilized with 0.2% Triton X-100 in PBS. After blocked with 1% BSA, cells were stained by incubation with primary antibodies (LC3) for 16 h at 4 °C. After washing, samples were incubated with Alexa Fluor 488-conjugated anti-mouse antibody. Cell nuclei were visualized with DAPI (Sigma). Slides were mounted with SlowFade Gold anti-fade reagent (Invitrogen), and detected under a LSM710 Laser Scanning Confocal Microscopy (Carl Zeiss).

2.6. Determination of cytokine and MPO levels

The levels of TNF-α, IL-6 and IL-1β in the culture supernatants or were measured by ELISA (R&D Systems). The lung MPO levels were determined using mouse MPO ELISA (Hycult Biotech) following the manufacturers' instructions.

2.7. Animal model

All of the animal experiments were performed in accordance with

the National Institutes of Health Guide for the Care and Use of Laboratory Animals [20], and with the approval of Animal Care and Use Committee of Nanjing University of Chinese medicine. BALB/c mice of 6–8 weeks of age were purchased from Model Animal Research Center of Nanjing University, and were housed under pathogen-free conditions on a 12/12 h light/dark cycle with free access to food and water. Mice were anesthetized intraperitoneally with ketamine hydrochloride (100 mg/kg) and xylazine (10 mg/kg).

For *S. aureus*-induced pneumonia, age- and sex-matched C57BL/6 mice (6 mice/group) were pretreated with DAPH (10 mg/kg, i.p.), vancomycin (100 mg/kg, i.p.) or with DMSO as a vehicle and then intratracheally challenged with *S. aureus* (5×10^6 CFU/mouse) or PBS. The animals were sacrificed 12 h later for the functional analysis. For bronchoalveolar lavage (BAL) and cell differentiation, BAL fluid (BALF) was obtained by flushing 3 times with 1 mL of 0.5 mM ethylenediaminetetraacetic acid/phosphate-buffered saline, and the supernatants were stored at −80 °C until use. Total cell numbers in BALF were counted with a hemocytometer, and differential cell counts were determined on cytospin preparations with Diff-Quick staining (International Medical Equipment). For determination of a survival curve, mice (10 mice/group) were injected with DAPH (10 mg/kg, i.p.) or DMSO 1 h before lethal dose of *S. aureus* infection (10^8 CFU/mouse). The percentage of survival rate was observed within 50 h post infection. The survival curve was plotted and analyzed with the Kaplan-Meier and log-rank statistic methods.

2.8. Phagocytosis assay

To assess the phagocytic capability of macrophages, CFSE-labeled *S. aureus* (MOI, 10) was incubated with macrophages for 0, 30, 60, 120 min. Infected cells were washed with PBS, and the uptake capability of the cells was quantified by flow cytometry.

2.9. Bactericidal assay

To determine the bactericidal capability of macrophages, the infected cells were further incubated in a fresh solution containing 2 μg/mL lysostaphin for the indicated periods. Alternatively, RAW264.7 cells (1×10^5) were infected with bacteria (MOI, 10). After 2–4 h, supernatants were collected, and cells were lysed to determine total viable bacterial loads. For immunofluorescence analysis of bacteria, RAW264.7 cells were grown on cover slips and incubated with *S. aureus* at indicated time points, cells were collected, fixed, and mounted in Vectashield with DAPI nuclear labeling (Invitrogen).

2.10. Real-time PCR

Total RNA was extracted from lung tissue or cell lysates using RNAprep Pure Tissue Kit (TIANGEN, DP431) and Trizol reagent (Invitrogen) respectively. cDNA was generated using an HiScript II One Step RT-PCR Kit (Vazyme, P612-01). SYBR Green PCR Master Mix (TOYOBO) was used to quantify mRNA levels. The reactions were performed in triplicate, and relative mRNA expression was determined by normalizing the expression of each target gene to that of β-actin using the $2^{-\triangle\triangle Ct}$ method.

2.11. Western blotting analysis

Total cell lysates were prepared using a lysis buffer containing 150 mM NaCl, 50 mM Tris-HCl (pH 7.4), 1% NP-40, and a cocktail of protease-inhibitors (Roche). A commercial kit for protein fractionation was purchased from Beyotime Institute of Biotechnology (cat # p0027). The proteins were separated by SDS-PAGE and transferred to PVDF membrane (Millipore). The proteins were detected by immunoblotting analysis using an ECL reagent kit (Millipore). β-actin was used as an internal control. The images were captured using ChemiDoc™ XRS$^+$ system (Bio-Rad, USA).

2.12. Hematoxylin and eosin (H&E) staining

Tissue samples were washed in PBS, fixed in 4% (*w/v*) formalin, and then paraffin embedded, sectioned, and stained with hematoxylin and eosin. The specimens were observed under a Leica inverted microscope DMi8 and photographed. Images were collected with 200× magnifications and processed using NIH ImageJ software.

2.13. Statistical analysis

Data were analyzed with GraphPad Software (SanDiego, CA). Statistical significance of differences was assessed with Student's *t*-test for two groups or one-way ANOVA for multiple groups. $P < 0.05$ values were considered significant. All independent parameters are mean ± SD of results in at least 3 independent experiments unless otherwise stated.

3. Results

3.1. DAPH confers protection against S. aureus-induced pneumonia

DAPH is a natural plant-derived agent with the chemical structure of 7, 8-dihydroxycoumarin. As revealed in our study, there was no apparent cytotoxic effect when applied at the dose up to 160 μM in cell culture system (Fig. 1A and B). Given its well-documented anti-microbial and anti-inflammatory properties, we thus set out to assess the potential role for DAPH in protecting against staphylococcal pneumonia. To this end, the sex-and age-matched mice were pre-instilled

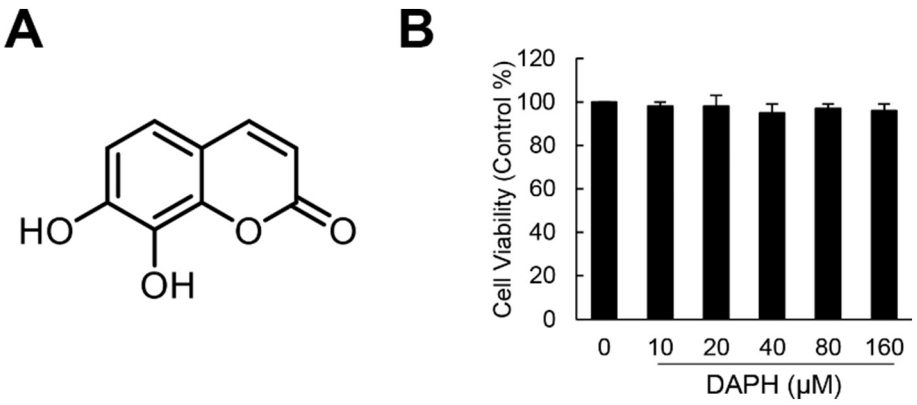

Fig. 1. Chemical structure and non-toxic effect of DAPH. (**A**) Chemical structure of DAPH. (**B**) Cell viability was analyzed by the CCK-8 assay in RAW264.7 cells treated with DAPH at the indicated dose for 48 h. Data represent the mean ± SD of three independent experiments.

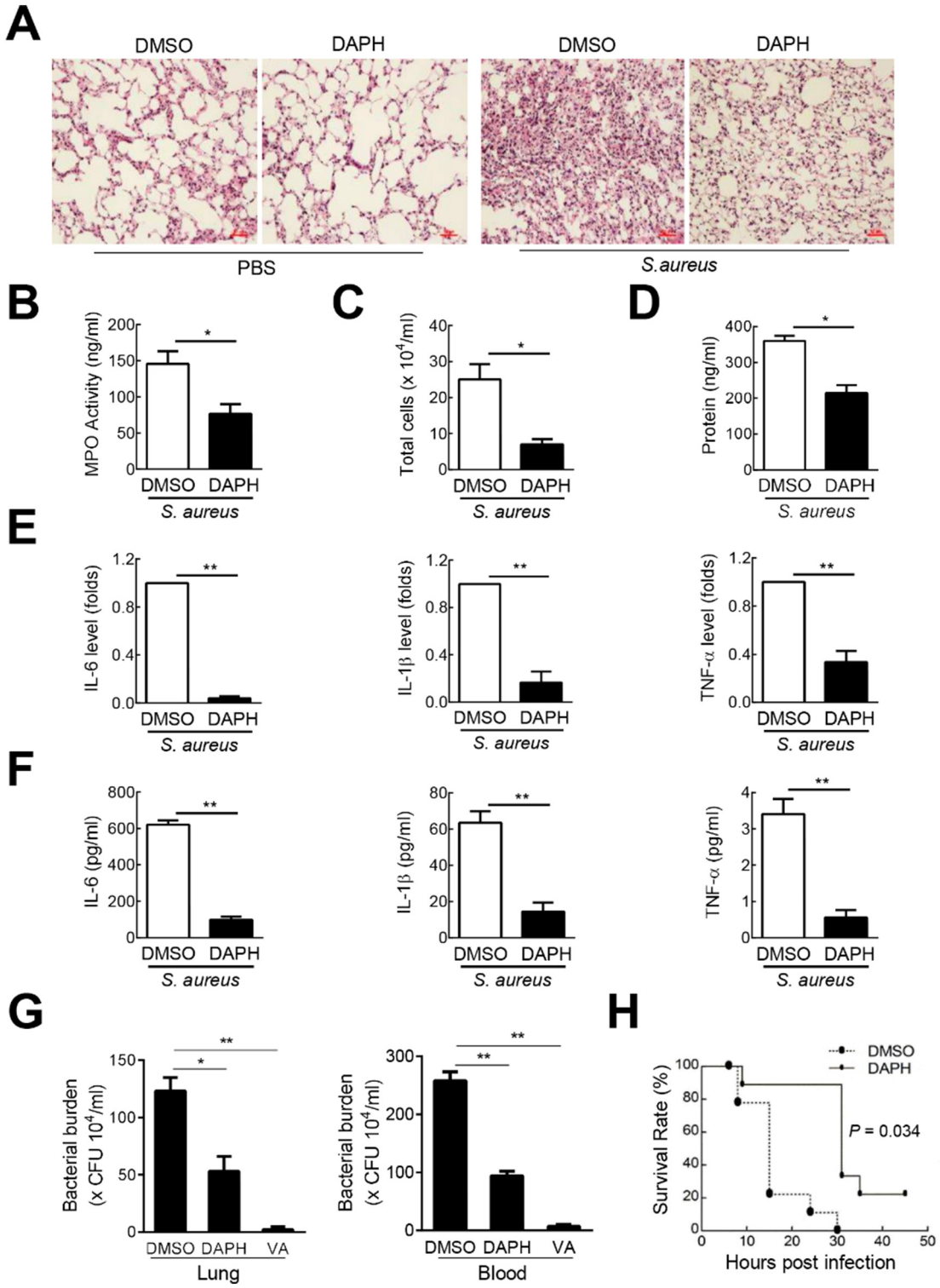

Fig. 2. DAPH renders the mice resistant to *S. aureus*-induced pneumonia. (**A–F**) Age- and sex-matched C57BL/6 mice (6 mice/group) were pretreated with DAPH (10 mg/kg, i.p.), vancomycin (100 mg/kg, i.p.) or with DMSO as a vehicle and then intratracheally challenged with *S. aureus* (5×10^6 CFU/mouse) or PBS. The animals were sacrificed 12 h later for the functional analysis. (**A**) Representative H&E staining of lung tissues. Original magnification, ×200; (**B**) BALF cell recovery; (**C**) MPO activity of lung tissues; (**D**) Protein concentration in BALF. (**E**) Proinflammatory cytokine levels in lung tissue; (**F**) BALF levels of proinflammatory cytokines. (**G**) Bacterial burden in lung tissue and blood. Vancomycin, as the standard drug. (**H**) Mice (10 mice/group) were injected with DAPH (10 mg/kg, i.p.) or DMSO 1 h before lethal dose of *S. aureus* infection (10^8 CFU/mouse). The survival curve was plotted and analyzed with the Kaplan-Meier and log-rank statistic methods. All results are expressed as the mean ± SD. * $P < 0.05$ and ** $P < 0.01$ by Student's *t*-test.

with DAPH (10 mg/kg, i.p.) or the vehicle for 30 min and then challenged with *S. aureus* (5×10^6 CFU/mouse, i.t.). The histopathological analysis reveal that, compared with the control group of animals, the mice pretreated with DAPH exhibited much lessened alveolar damage and inflammapathology, characterized by the reduced interstitial edema and debris deposit, less inflammatory cell infiltration and more organized lung tissues (Fig. 2A). In agreement with this, BALF cellular amounts and lung MPO activity, the indicative of neutrophil infiltration, were decreased upon DAPH treatment (Fig. 2B and C). Also, the protein leakage into the BALF and the production of pro-inflammatory cytokines including IL-6, TNF-α, and IL-1β were repressed by DAPH administration (Fig. 2D–F). Critically, our data showed that bacterial burden, either in lung tissues or in peripheral blood was significantly reduced in DAPH-treated mice (Fig. 2G). Consequently, the mice treated with DAPH exhibited significantly prolonged survival compared with their control littermates when challenged with lethal dose (10^8 CFU/mouse, i.t.) of *S. aureus* (Fig. 2H). Collectively, our data demonstrated that DAPH conferred a profound protection against bacterial pneumonia caused by the formidable MRSA.

3.2. DAPH negatively regulates the inflammatory response induced by S. aureus infection

Since macrophages constitute the major cellular components required for anti-bacterial innate immune and inflammatory responses, we then set to assess the effect of DAPH on macrophage response to staphylococcal infection. We expectedly found that the challenge of macrophages with *S. aureus* led to a remarkable production of pro-inflammatory cytokines, including IL-6, TNF-α, and IL-1β, either at the mRNA and protein levels. Strikingly, our data indicated that the treatment of DAPH, in a time-dependent manner, repressed the expression of proinflammatory cytokines induced by *S. aureus* (Fig. 3A, B). We also found that DAPH significantly repressed the expression of inducible nitric-oxide synthase (iNOS), the enzyme required for the production of pro-inflammatory NO (Fig. 3C). Thus, DAPH treatment appeared to exert the negative effect on the production of proinflammatory cytokines induced by *S. aureus* infection.

To understand the mechanism underlying DAPH-mediated control of production of proinflammatory cytokines, we next analyzed its impact on activity of key signaling molecules such as NF-κB and mitogen-activated protein kinase (MAPKs). As shown in Fig. 4A, the activation of NF-κB pathway, as revealed by the phosphorylation of p65 and its upstream signaling molecules inhibitor of nuclear factor kappa-B kinase (IκB)α and IκB kinase (IKK), were reduced upon DAPH treatment in *S. aureus*-infected macrophages (Fig. 4A). Consistent with these results, NF-κB-driven promoter activity was also repressed by DAPH in a dose-dependent manner (Fig. 4B). Additionally, we detected the activity of major MAPKs such as JNK, ERK, and p38, which have been proved to be essential for the inflammatory response in the infected cells. The result showed that pretreatment of DAPH reduced phosphorylation of JNK, ERK, and p38 kinases induced by *S. aureus* stimulation (Fig. 4C). We thus concluded that DAPH repressed the activation of key signaling pathways essential for the expression of pro-inflammatory mediators, that might be partially at least, responsible for its anti-inflammatory property.

3.3. DAPH treatment enhances macrophage bactericidal activity

Given the observation that the administration of DAPH significantly reduced bacterial loads in murine model of staphylococcal pneumonia, we asked whether DAPH affected the capability of macrophages to constrain bacterial infection. Because the phagocytosis and internalizing of the invading pathogens constituted the first step for infection control, we thus initially tested the phagocytic ability of macrophages with or without DAPH treatment. To this end, RAW264.7 cells were subject to CFSE-labeled *S. aureus* infection, and the percentage of cells with internalized bacteria was examined by flow cytometry. The result showed that the treatment of DAPH excreted no apparent effect on the amount of the internalized bacteria, indicating that macrophage phagocytic capability was not significantly affected by DAPH treatment (Fig. 5A). Next, we evaluated macrophage bactericidal activity using the lysostaphin protection assay, the well-recognized experiment used to determine the survival of intracellular bacteria a period of time following pathogens exposure. Critically, our data showed that the amounts of labeled bacteria, as detected by fluorescence microscopy, were significantly reduced in macrophages pretreated with DAPH

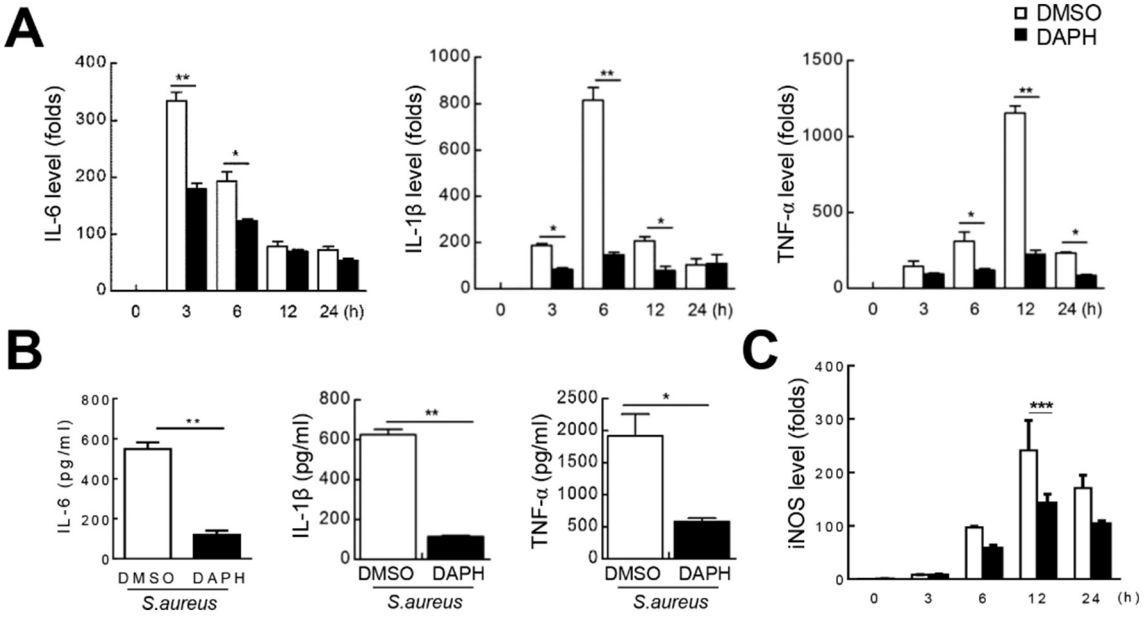

Fig. 3. DAPH inhibits the production of pro-inflammatory cytokines induced by *S. aureus* infection. (**A–C**) RAW264.7 cells were pretreated with DMSO or DAPH (160 μM) for 30 min followed by the infection of *S. aureus* (MOI, 10) for the indicated time periods. Expression of IL-6, IL-1β, and TNF-α at mRNA level (**A**), and protein level (**B**) was determined by qPCR or ELISA, respectively; and the expression of iNOS was analyzed qPCR (**C**). Data are the mean ± SD of three independent experiments. $* P < 0.05$ and $** P < 0.01$ by Student's *t*-test.

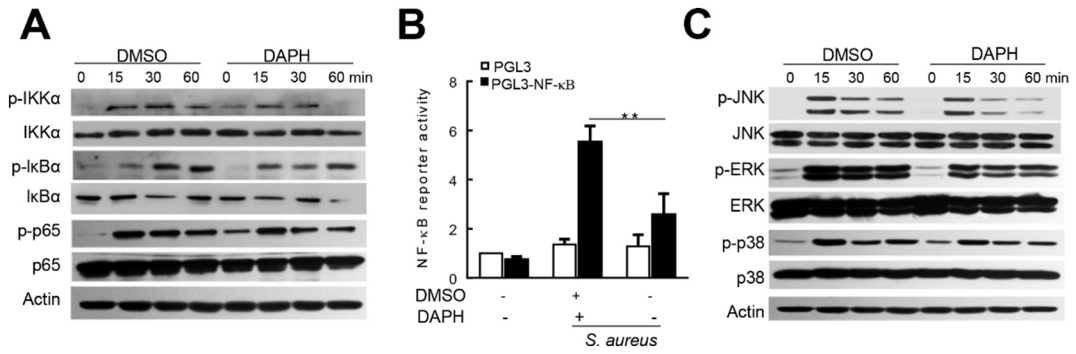

Fig. 4. DAPH represses the inflammatory signaling induced by *S. aureus*. (**A–C**) RAW264.7 cells were pretreated with either DMSO or DAPH (160 μM) 30 min prior to *S. aureus* stimulation. Levels of the major signaling molecules involved in the activation of NF-κB (**A**) and MAPKs (**C**) were detected by immunoblotting, and the NF-κB-driven promoter activity was analyzed by the dual luciferase assay (**B**). Data are the mean ± SD of three independent experiments. $^{*}P < 0.05$ and $^{**}P < 0.01$ by Student's *t*-test. Results are representative of three individual experiments.

(Fig. 5B). Consistent with this, the assay for viable bacteria loads by the plate-dilution method revealed that bacterial burden in DAPH-treated macrophages was significantly reduced compared with that in control cells (Fig. 5B). The results thus supported that DAPH treatment significantly enhanced macrophage bactericidal but not phagocytic capability. Intriguingly, our data showed that the level of reactive oxygen species (ROS), as measured with DCFH-DA fluorescent probe, was decreased in DAPH-treated macrophages, implying a protective role of DAPH against oxidative stress during staphylococcal infection (Fig. 5C).

3.4. DAPH treatment enhances the autophagic pathway essential for anti-bacterial and anti-inflammatory activity

Cellular autophagy is known to have important roles in the

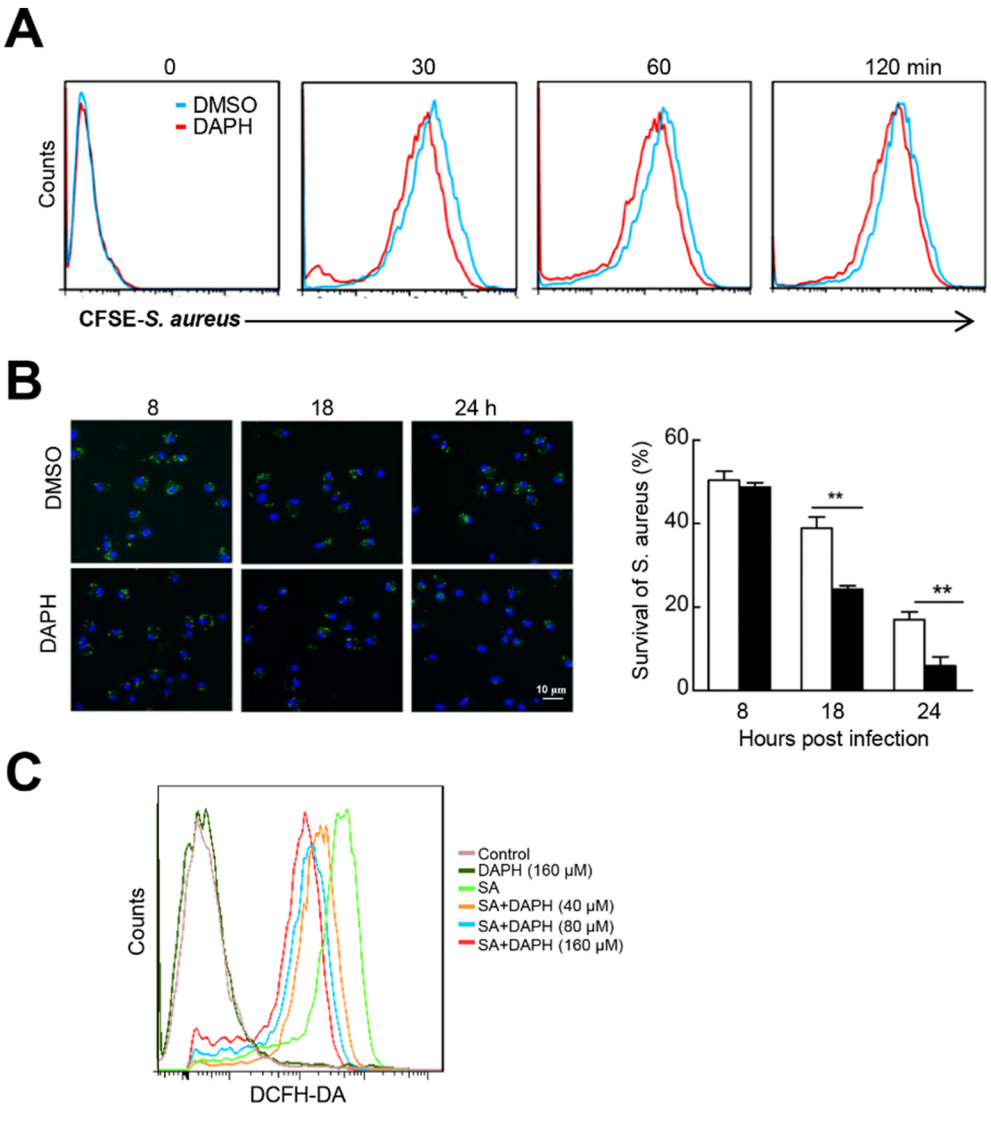

Fig. 5. DAPH enhances macrophage bactericidal activity while suppressing ROS production. (**A**) Uptake of CFSE-labeled *S. aureus* was quantified using flow cytometry. RAW264.7 cells were pretreated with DAPH or DMSO for 30 min and incubated with bacteria for 30, 60 and 120 min, followed by the analysis of the rates of fluorescence positivity. Representative traces of engulfed bacteria are indicated by red (DMSO) and blue line (DAPH), respectively. (**B**) Survival of the intracellular *S. aureus* was detected by immunofluorescence microscopy (left), and total viable bacteria were quantified by the plate-dilution culture (right) at 8, 18 and 24 h post infection. Representative images of 3 samples per group are depicted. Nuclei are stained with DAPI (blue); CFSE-labeled *S. aureus* appeared green (original magnification, ×20). (**C**) Evaluation of ROS generation using DCFH-DA fluorescent probe in RAW264.7 cells with or without Staphylococcal infection. (For interpretation of the references to color in this figure legend, the reader is referred to the web version of this article.)

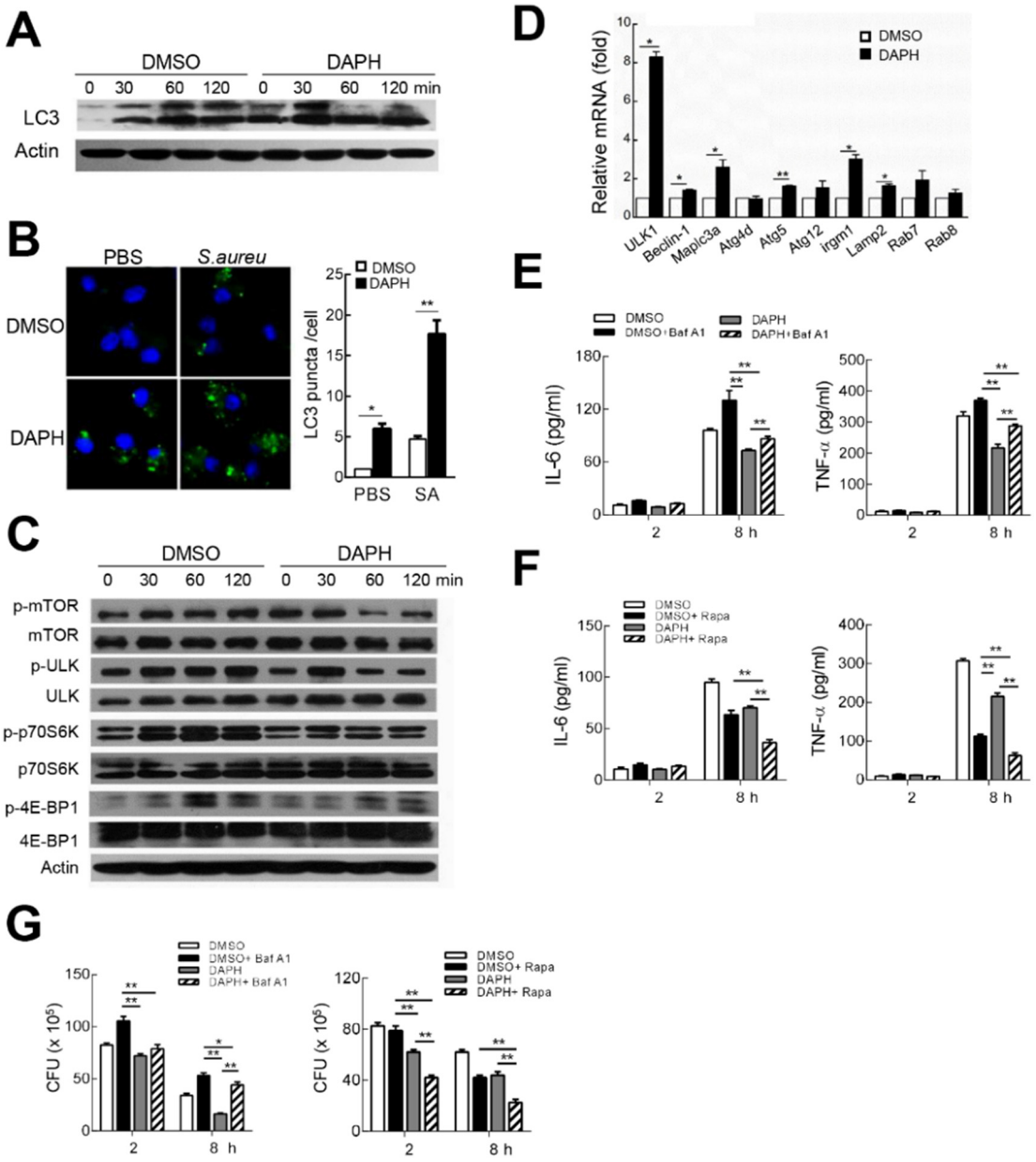

Fig. 6. DAPH promotes the anti-bacterial autophagy through regulating mTOR pathway. (**A–E**) RAW264.7 cells were pretreated with either DMSO or DAPH (160 μM) 30 min prior to Staphylococcal infection. Western-blotting of LC3 I/II level (**A**). Representative confocal images and quantification of LC3 puncta (**B**); Western-blotting of the level of mTOR-related signaling molecules (**C**); qPCR analysis of the expression of autophagy-lysosome genes (**D**). (**E–G**) RAW264.7 cells were pretreated with DMSO or DAPH, along with the addition of Baf-A1 or Rapamycin (Rapa) respectively for 30 min. Cells were then challenged with *S. aureus* for the indicated time periods. IL-6 and TNF-α were examined by ELISA (**E**, **F**), and bacterial loads were enumerated using plate-dilution methods (**G**).

elimination of intracellular microorganisms and the modulation of inflammation. To further understand the action mode of DAPH during staphylococcal infection, we next analyzed the potential role of DAPH in autophagic response induced by *S. aureus*. Indeed, the conversion of LC3-I to LC3-II, one of the most prominent features of autophagic process, was significantly enhanced by DAPH treatment in *S. aureus*-infected macrophages (Fig. 6A). The result was in agreement with the increased amplitude of LC3 puncta observed in these cells (Fig. 6B). We next assessed the activity of mammalian target of rapamycin (mTOR), the serine/threonine kinase known to have an inhibitory role in autophagic pathway. Remarkably, the results showed that the activation of mTOR, along with its downstream signaling molecules including unc-51 like kinase (ULK)1, ribosomal protein S6 kinases (p70S6K) and eukaryotic translation initiation factor 4*E*-binding protein 1 (4E-BP1), was repressed upon DAPH treatment in bacteria-stimulated macrophages (Fig. 6C), indicating the de-repression of the autophagic pathway upon DAPH treatment in these cells. Consequentially, the expression of autophagy-lysosome genes were up-regulated in DAPH-treated macrophages compared with that in control cells (Fig. 6D).

To further confirm the functional relevance of DAPH-mediated regulation of autophagic process in anti-bacterial response, we then utilized Bafilomycin A1 (Baf-A1), a putative autophagy inhibitor, to block autophagic flux in bacteria-challenged macrophages. The result showed that the decreased production of IL-6 and TNF-α, as well as the lessened bacterial burden caused by DAPH treatment was largely abrogated upon Baf-A1 treatment (Fig. 6E and G). In contrast, the application of Rapamycin, the canonical mTOR inhibitor and hence an inducer of autophagy, reduced IL-6 and TNF-α levels, and bacterial loads in vehicle-treated macrophages, which however exerted slight effects on DAPH-treated cells (Fig. 6F and G). Collectively, our data indicated

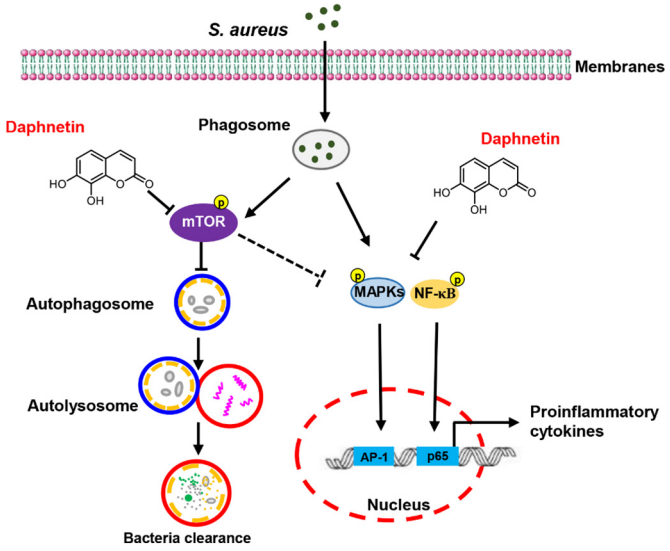

Fig. 7. Schematic summary of DAPH-mediated regulation of anti-bacterial and anti-inflammatory responses.

that DAPH potentially enhanced mTOR-dependent autophagic pathway, inhibition of which likely abrogated the regulatory effect of DAPH during Staphylococcal infection (Fig. 7).

4. Discussion

Daphnetin is a coumarin derivative that has been documented to possess multiple pharmacological including analgesia, antimalarial, anti-arthritic, and anti-pyretic properties. It also exerts the anti-inflammatory and anti-oxidative effects presumably through inhibiting the production of proinflammatory lipoxygenase and reducing the activity of lipid peroxidation and glutathione reductases [21,22]. Accumulating data have demonstrated that either the extracted or the synthetic coumarin derivatives exhibited antibacterial activity against a variety of bacterium such as *Bacillus lentus*, *Escherichia coli*, *Ralstonia solanacearum and Pseudomonas aeruginosa* [23,24]. Mechanistically, the compounds displayed to retard microorganism growth and hinder the synthesis of virulent factors like pyocyanin, biofilm and elastase [25,26]. Daphnetin has been listed as one of the most active compounds with anti-microbial property, but the underlying mechanism was largely unknown. Our present study demonstrates that DAPH potentially enhanced the mTOR-dependent autophagic pathway in macrophages, leading to the lessened bacterial burden and the alleviated inflammapathology and thereby conferring the protection against staphylococcal pneumonia in mice. To our knowledge, this is the first report that coumarin derivate serves as an autophagic modulator and hence as a potential controller of bacterial infection, which might provide novel insights into action mode of coumarin, and more importantly, into the development of new anti-microbial therapeutics, especially for obstinate pathogens such as MRSA.

MRSA has been recognized as a major cause of community-acquired pneumonia and a leading cause of healthcare-associated pneumonia [27,28]. Despite many efforts invested in treating staphylococcal infection, the increasing prevalence of antibiotic-resistant strains make it one of the most deadly diseases worldwide [29,30]. The failure to develop new antibiotics in recent years renders the investigators turn to the strategy aimed to modify host defensive system [31,32]. Macrophages are the first line to combat bacterial infection, which are proposed to be rapidly recruited during *S. aureus* infection, sense the invading pathogens, elicit innate inflammatory response, and induce adaptive immune response when necessary [33]. Effective induction of macrophage responses is crucial for bacterial containment. However, the associated release of proinflammatory cytokines and chemokines propagates the inflammatory signaling and attracts more inflammatory cells, leading to the unwanted inflammation and extensive tissue damage. Therefore, the coordination of anti-bacterial and anti-inflammatory response holds the key for successful control of infectious diseases [34].

Autophagy is a conservative cellular degradative system and also homeostatic mechanism that plays an essential role in defensing against pathogen invasion [35–37]. The internalized bacteria within macrophages demonstrate to be sequestrated in autophagosomes and ultimately delivered to the lysosomes for degradation. In this study, we found that DAPH promoted the conversion of LC3-I to LC3-II and the formation of LC3 puncta in *S. aureus*-challenged macrophages, indicating the boosted effect of DAPH in autophagic pathway. In parallel, DAPH treatment significantly inhibited the activation of mTOR and the downstream signaling pathway, which would subsequently de-repress the transcription factor EB (TFEB), and hence trigger the expression of autolysosomal genes. We thus observed that the expression of the representative autolysosomal genes was remarkably augmented upon DAPH treatment. Although the detailed mechanism involved in this process needs further investigation, our study uncovers a novel mechanism that was utilized by DAPH to combat staphylococcal infection. To be supportive, the blocking of autophagic flux in macrophages resulted in higher bacterial burden and the aggravated inflammatory response, whereas the induction of autophagic signaling by the inhibition of mTOR mimics the action of DAPH. The results thus highlighted the importance of autophagy in orchestrating the anti-bacterial and anti-inflammation activity and suggest a novel perspective on the treatment of critical infectious diseases which are frequently intertwined with infection and inflammation. In this regarding, the potential synergism of DAPH in both suppressing NF-κB and MAPKs, and mTOR activity merits further investigation.

Intriguingly, previous study indicated that *S. aureus* localized to autophagosomes, which was believed to inhibit the maturation and lysosome-fusion of autophagosomes, and the subsequent bacterial lysis. The results implied that the interference of autophagic pathway might be used by pathogens to evade the clearance and make them survive intracellularly, which likely lend additional support for our present observation that autophagy-targeting agents might be more effective for containing the refractory infection [38–40]. Additionally, studies have shown that excessive autophagy occurring in host tissues might generate the so-called “autophagic cell death” and lead to the detrimental cellular damage. Thus, calibrating the net costs of autophagic responses during bacterial infection is of significance.

Together, our current study identify an essential role for autophagy in controlling the clinically refractory bacterial and highlight the potential of natural, plant-derived compounds in treating bacterial pneumonia.

Conflict of interest statement

The authors declare no competing financial interests.

Acknowledgments

This work was supported by National Natural Scientific Funds (81470210 and 81770014), National Key R&D Program of China (2018YFC 1705900), Natural Science Foundation of Jiangsu Province Fund (BK20180824), and a project funded by the Priority Academic Program Development of Jiangsu Higher Education Institutions.

Author contributions

LS designed experiments. WZ, SZ, LH, and CC performed experiments; WZ and BZ analyzed data. WZ and LS wrote the manuscript. YL, QW, WG and WS contributed to experimental material and suggestions.

LS supervised the research.

References

[1] I. Inoshima, N. Inoshima, G.A. Wilke, M.E. Powers, K.M. Frank, Y. Wang, J. Bubeck Wardenburg, A Staphylococcus aureus pore-forming toxin subverts the activity of ADAM10 to cause lethal infection in mice, Nat. Med. 17 (10) (2011) 1310–1314.

[2] M.B. Mestre, C.M. Fader, C. Sola, M.I. Colombo, Alpha-hemolysin is required for the activation of the autophagic pathway in Staphylococcus aureus-infected cells, Autophagy 6 (1) (2010) 110–125.

[3] K. Haapasalo, A.J.M. Wollman, C.J.C. de Haas, K.P.M. van Kessel, J.A.G. van Strijp, M.C. Leake, Staphylococcus aureus toxin LukSF dissociates from its membrane receptor target to enable renewed ligand sequestration, FASEB J. 33 (3) (2019) 3807–3824.

[4] M. Otto, A MRSA-terious enemy among us: end of the PVL controversy? Nat. Med. 17 (2) (2011) 169–170.

[5] A.Y. Meliton, F. Meng, Y. Tian, N. Sarich, G.M. Mutlu, A.A. Birukova, K.G. Birukov, Oxidized phospholipids protect against lung injury and endothelial barrier dysfunction caused by heat-inactivated Staphylococcus aureus, Am. J. Phys. Lung Cell. Mol. Phys. 308 (6) (2015) L550–L562.

[6] J. Kaur, J. Debnath, Autophagy at the crossroads of catabolism and anabolism, Nat. Rev. Mol. Cell Biol. 16 (8) (2015) 461–472.

[7] N. Mizushima, M. Komatsu, Autophagy: renovation of cells and tissues, Cell 147 (4) (2011) 728–741.

[8] J. Wang, K. Yang, L. Zhou, Y. Wu Minhaowu, M. Zhu, X. Lai, T. Chen, L. Feng, M. Li, C. Huang, Q. Zhong, X. Huang, MicroRNA-155 promotes autophagy to eliminate intracellular mycobacteria by targeting Rheb, PLoS Pathog. 9 (10) (2013) e1003697.

[9] E.F. Castillo, A. Dekonenko, J. Arko-Mensah, M.A. Mandell, N. Dupont, S. Jiang, M. Delgado-Vargas, G.S. Timmins, D. Bhattacharya, H. Yang, J. Hutt, C.R. Lyons, K.M. Dobos, V. Deretic, Autophagy protects against active tuberculosis by suppressing bacterial burden and inflammation, Proc. Natl. Acad. Sci. U. S. A. 109 (46) (2012) E3168–E3176.

[10] K. Cadwell, Crosstalk between autophagy and inflammatory signalling pathways: balancing defence and homeostasis, Nat. Rev. Immunol. 16 (11) (2016) 661–675.

[11] P. Jiang, N. Mizushima, Autophagy and human diseases, Cell Res. 24 (1) (2014) 69–79.

[12] T. Shintani, D.J. Klionsky, Autophagy in health and disease: a double-edged sword, Science 306 (5698) (2004) 990–995.

[13] J.J. Kim, H.M. Lee, D.M. Shin, W. Kim, J.M. Yuk, H.S. Jin, S.H. Lee, G.H. Cha, J.M. Kim, Z.W. Lee, S.J. Shin, H. Yoo, Y.K. Park, J.B. Park, J. Chung, T. Yoshimori, E.K. Jo, Host cell autophagy activated by antibiotics is required for their effective antimycobacterial drug action, Cell Host Microbe 11 (5) (2012) 457–468.

[14] M. Li, X. Shi, F. Chen, F. Hao, Daphnetin inhibits inflammation in the NZB/W F1 systemic lupus erythematosus murine model via inhibition of NF-kappaB activity, Exp. Ther. Med. 13 (2) (2017) 455–460.

[15] A. Kumar, S. Jha, S.P. Pattanayak, Daphnetin ameliorates 7,12-dimethylbenz[a] anthracene-induced mammary carcinogenesis through Nrf-2-Keap1 and NF-kappaB pathways, Biomed. Pharmacother. 82 (2016) 439–448.

[16] W.W. Yu, Z. Lu, H. Zhang, Y.H. Kang, Y. Mao, H.H. Wang, W.H. Ge, L.Y. Shi, Anti-inflammatory and protective properties of daphnetin in endotoxin-induced lung injury, J. Agric. Food Chem. 62 (51) (2014) 12315–12325.

[17] R. Yao, Y. Fu, S. Li, L. Tu, X. Zeng, N. Kuang, Regulatory effect of daphnetin, a coumarin extracted from Daphne odora, on the balance of Treg and Th17 in collagen-induced arthritis, Eur. J. Pharmacol. 670 (1) (2011) 286–294.

[18] L. Tu, S. Li, Y. Fu, R. Yao, Z. Zhang, S. Yang, X. Zeng, N. Kuang, The therapeutic effects of daphnetin in collagen-induced arthritis involve its regulation of Th17 cells, Int. Immunopharmacol. 13 (4) (2012) 417–423.

[19] D. Wang, Z. Lu, H. Zhang, S.F. Jin, H. Yang, Y.M. Li, L.Y. Shi, Daphnetin alleviates experimental autoimmune encephalomyelitis via regulating dendritic cell activity, CNS Neurosci. Ther. 22 (7) (2016) 558–567.

[20] Guide for the Care and Use of Laboratory Animals, Washington (DC), (2011).

[21] L. Shen, T. Zhou, J. Wang, X. Sang, L. Lan, L. Luo, Z. Yin, Daphnetin reduces endotoxin lethality in mice and decreases LPS-induced inflammation in Raw264.7 cells via suppressing JAK/STATs activation and ROS production, Inflamm. Res. 66 (7) (2017) 579–589.

[22] A. Witaicenis, L.N. Seito, A. da Silveira Chagas, L.D. de Almeida Jr., A.C. Luchini, P. Rodrigues-Orsi, S.H. Cestari, L.C. Di Stasi, Antioxidant and intestinal anti-inflammatory effects of plant-derived coumarin derivatives, Phytomedicine 21 (3) (2014) 240–246.

[23] R.E. D'Almeida, R.D.I. Molina, C.M. Viola, M.C. Luciardi, C. Nieto Penalver, A. Bardon, M.E. Arena, Comparison of seven structurally related coumarins on the inhibition of Quorum sensing of Pseudomonas aeruginosa and Chromobacterium violaceum, Bioorg. Chem. 73 (2017) 37–42.

[24] Y. Zhang, A. Sass, H. Van Acker, J. Wille, B. Verhasselt, F. Van Nieuwerburgh, V. Kaever, A. Crabbe, T. Coenye, Coumarin reduces virulence and biofilm formation in Pseudomonas aeruginosa by affecting quorum sensing, type III secretion and C-di-GMP levels, Front. Microbiol. 9 (2018) 1952.

[25] S.M.F.L. da, T.Q. Froes, M.F.C. Cardoso, C.A. de Oliveira Maciel, G.G. Nicastro, R.L. Baldini, D.C.S. Costa, V.F. Ferreira, M.S. Castilho, C.d.S.F. de, Synthesis and biological evaluation of Coumarins derivatives as potential inhibitors of the production of Pseudomonas aeruginosa virulence factor pyocyanin, Curr. Top. Med. Chem. 18 (2) (2018) 149–156.

[26] F.J. Reen, J.A. Gutierrez-Barranquero, M.L. Parages, O.G. F, Coumarin: a novel player in microbial quorum sensing and biofilm formation inhibition, Appl. Microbiol. Biotechnol. 102 (5) (2018) 2063–2073.

[27] A.C. Uhlemann, M. Otto, F.D. Lowy, F.R. DeLeo, Evolution of community- and healthcare-associated methicillin-resistant Staphylococcus aureus, Infect. Genet. Evol. 21 (2014) 563–574.

[28] R.S. Daum, Clinical practice. Skin and soft-tissue infections caused by methicillin-resistant Staphylococcus aureus, N. Engl. J. Med. 357 (4) (2007) 380–390.

[29] A.S. Fauci, D. Marston l, The perpetual challenge of antimicrobial resistance, JAMA 311 (18) (2014) 1853–1854.

[30] B. Spellberg, J.G. Bartlett, D.N. Gilbert, The future of antibiotics and resistance, N. Engl. J. Med. 368 (4) (2013) 299–302.

[31] L. Czaplewski, R. Bax, M. Clokie, M. Dawson, H. Fairhead, V.A. Fischetti, S. Foster, B.F. Gilmore, R.E. Hancock, D. Harper, I.R. Henderson, K. Hilpert, B.V. Jones, A. Kadioglu, D. Knowles, S. Olafsdottir, D. Payne, S. Projan, S. Shaunak, J. Silverman, C.M. Thomas, T.J. Trust, P. Warn, J.H. Rex, Alternatives to antibiotics-a pipeline portfolio review, Lancet Infect. Dis. 16 (2) (2016) 239–251.

[32] B. Park, G.Y. Liu, Targeting the host-pathogen interface for treatment of Staphylococcus aureus infection, Semin. Immunopathol. 34 (2) (2012) 299–315.

[33] L.C. Chan, M. Rossetti, L.S. Miller, S.G. Filler, C.W. Johnson, H.K. Lee, H. Wang, D. Gjertson, V.G. Fowler Jr., E.F. Reed, M.R. Yeaman, M.S.I. Group, Protective immunity in recurrent Staphylococcus aureus infection reflects localized immune signatures and macrophage-conferred memory, Proc. Natl. Acad. Sci. U. S. A. 115 (47) (2018) E11111–E11119.

[34] X. Jiang, Y. Wang, Y. Qin, W. He, A. Benlahrech, Q. Zhang, X. Jiang, Z. Lu, G. Ji, Y. Zheng, Micheliolide provides protection of mice against Staphylococcus aureus and MRSA infection by down-regulating inflammatory response, Sci. Rep. 7 (2017) 41964.

[35] B. Levine, G. Kroemer, Autophagy in the pathogenesis of disease, Cell 132 (1) (2008) 27–42.

[36] K. Yuan, C. Huang, J. Fox, D. Laturnus, E. Carlson, B. Zhang, Q. Yin, H. Gao, M. Wu, Autophagy plays an essential role in the clearance of Pseudomonas aeruginosa by alveolar macrophages, J. Cell Sci. 125 (Pt 2) (2012) 507–515.

[37] S. Chauhan, M.A. Mandell, V. Deretic, IRGM governs the core autophagy machinery to conduct antimicrobial defense, Mol. Cell 58 (3) (2015) 507–521.

[38] A. Chong, T.D. Wehrly, R. Child, B. Hansen, S. Hwang, H.W. Virgin, J. Celli, Cytosolic clearance of replication-deficient mutants reveals Francisella tularensis interactions with the autophagic pathway, Autophagy 8 (9) (2012) 1342–1356.

[39] M. Ogawa, T. Yoshimori, T. Suzuki, H. Sagara, N. Mizushima, C. Sasakawa, Escape of intracellular Shigella from autophagy, Science 307 (5710) (2005) 727–731.

[40] Y. Yoshikawa, M. Ogawa, T. Hain, M. Yoshida, M. Fukumatsu, M. Kim, H. Mimuro, I. Nakagawa, T. Yanagawa, T. Ishii, A. Kakizuka, E. Sztul, T. Chakraborty, C. Sasakawa, Listeria monocytogenes ActA-mediated escape from autophagic recognition, Nat. Cell Biol. 11 (10) (2009) 1233–1240.